An Acad Bras Cienc (2023) 95(Suppl. 3): e20230283 DOI 10.1590/0001-3765202320230283
Anais da Academia Brasileira de Ciências | *Annals of the Brazilian Academy of Sciences*
Printed ISSN 0001-3765 I Online ISSN 1678-2690
www.scielo.br/aabc | www.fb.com/aabcjournal

GEOSCIENCES

Low numbers of large microplastics on environmentally-protected Antarctic beaches reveals no widespread contamination: insights into beach sedimentary dynamics

CAIK O. DE MIRANDA, CARLOS ERNESTO G.R. SCHAEFER, JOSÉ JOÃO L.L. DE SOUZA, LUCIANO M. GUIMARÃES, PAULO VICTOR S. MAIA & JULIANA A. IVAR DO SUL

Abstract: Microplastics are ubiquitous contaminants of marine ecosystems around the world and Antarctica is no exception. Microplastics can be influenced by sedimentary dynamics mainly on coastal areas where they are more abundant in Antarctica. This study evaluated microplastic contamination in beach environments from two Antarctic Specially Protected Areas, aiming to identify relationships between microplastic numbers and sedimentological parameters on beach sediments. Low numbers of microplastics were found (> 0.5 mm; fibers excluded) – one particle per sample in 4 of 15 samples analyzed – and there is no evidence of widespread contamination. Sedimentological parameters reveal differences between sampled environments, but low numbers of microplastics impaired statistical comparison. All sediment samples are coarse, denoting high-energy depositional environments that are likely little susceptible to microplastic accumulation. Microplastic contamination in the Antarctic coastal ecosystem is heterogeneous, and their detailed characterization assisted by a systematization of methods can improve the understanding of microplastics distribution patterns in the cold coastal ecosystem.

Key words: Antarctic Specially Protected Areas, raman spectroscopy, sedimentary dynamics, South Shetlands Islands, stranded plastics.

INTRODUCTION

Microplastics (MPs) are plastic particles (0.001-5 mm in size) with a myriad of shapes that are intentionally produced by industry (primary-MP) or are fragments from larger plastics (secondary-MP) (Frias et al. 2018, Hidalgo-Ruz et al. 2012). MPs are ubiquitous contaminants of the marine ecosystem worldwide, as documented by extensive research in the last decades (e.g. Ajith et al. 2020, Lebreton et al. 2019). Although geographically isolated and protected by international law, the Antarctic continent is no exception (Caruso et al. 2022).

The Protocol on Environmental Protection to the Antarctic Treaty, since 1998, as a principle seeks the integral protection and preservation of the Antarctic ecosystem, reinforcing its value as an area designated for scientific research only (Committee of Environmental Protection 1991b). The protocol defines Antarctic Specially Protected Areas (ASPAs), which are endowed with geographical and environmental singularities and should be protected from human interference (Committee of Environmental Protection 1991a). For example, ASPAs 128 and 126, located in South Shetlands Islands, Maritime Antarctica, are sensitive to climate change and present extensive ice-free areas where periglacial processes occur (López-Martínez et al. 2012). Both ASPAs are home to fauna and flora representative of the Maritime Antarctica ecosystem (ATCM 2014, 2016), and the expansion of ice-free areas, mostly in recent years, promotes the formation of new landscapes that affect their occupation (Francelino et al. 2011).

Evidence of plastic contamination in the Antarctic ecosystem dates back to the 1980s, by the reported ingestion of plastics by Antarctic seabirds (van Franeker & Bell 1988). However, recent studies reported the presence of MPs everywhere, including the Southern Ocean (Absher et al. 2019, Isobe et al. 2017, Lacerda et al. 2019), sediments (Reed et al. 2018, Waller et al. 2017), sea ice (Kelly et al. 2020), freshwater (González-Pleiter et al. 2020) and marine vertebrates (Fragão et al. 2021, Le Guen et al. 2020) and invertebrates (Sfriso et al. 2020). Human activities carried out below 60° South have been pointed to as potential endogenous sources of plastics (Cincinelli et al. 2017, Lacerda et al. 2019, Munari et al. 2017). Exogenous sources can also be significant because MPs can be trapped and eventually accumulate within the Polar Front and Antarctic Circumpolar Current (ACC) (Isobe et al. 2017, Lacerda et al. 2019). Although the abundance of MPs in the open Southern Ocean is often lower than those reported in other parts of the globe, their prevalence near coastal areas is representative (Kuklinski et al. 2019, Tirelli et al. 2020), however MPs assessments on the Antarctic beaches are still little explored.

In coastal areas, MPs are components of sedimentary dynamics (Enders et al. 2019, Vianello et al. 2013, Zalasiewicz et al. 2016), opening a range of avenues to be explored within sedimentology, morphodynamics, and other related research lines. MPs amounts are influenced by the distance from sources of contamination to the sinking area and also by energetic dynamics acting within the sedimentary environments, which reflects in the granulometry of the sediment (Enders et al. 2019, Mendes et al. 2021). Grain size and sorting reflect depositional processes and the evolution of coastal sedimentary environments (Edwards 2001, Folk 1966), and give important clues about MP-sediment dynamics. For example, MPs are highly correlated with fine fractions of beach sediments (Enders et al. 2019, Mendes et al. 2021). Coastal areas of the Maritime Antarctic region are subject to severe conditions of marine dynamics and represent mostly high-energy depositional environments (Chereskin et al. 2009, Kejna et al. 2013, do Vale Lopes et al. 2022), which can hamper MPs deposition, but studies on sedimentological parameters and sedimentary dynamics of modern beaches are scarce.

This study aimed to evaluate MP contamination in beaches and coastal areas occupied by Antarctic marine fauna of two terrestrial ASPA of the Maritime Antarctica region. In addition, we evaluated sedimentological parameters of the sampled environments to assess relationships to help understand the dynamics of MPs in Maritime Antarctic beach ecosystems. We hypothesized these coast environments would have representative MP contents given the evidence of MP presence and their dispersion across the Southern Ocean, and their beach depositional compartments would have different sedimentary dynamics that may influence the presence of MPs.

Study area

ASPA 128

The ASPA 128 (16.8 km^2, 58º27’40” W, 62º11’50” S) is located in King George Island, South Shetlands Archipelago, on the west face of the entrance to Admiralty Bay (Figure 1). The Admiralty Bay

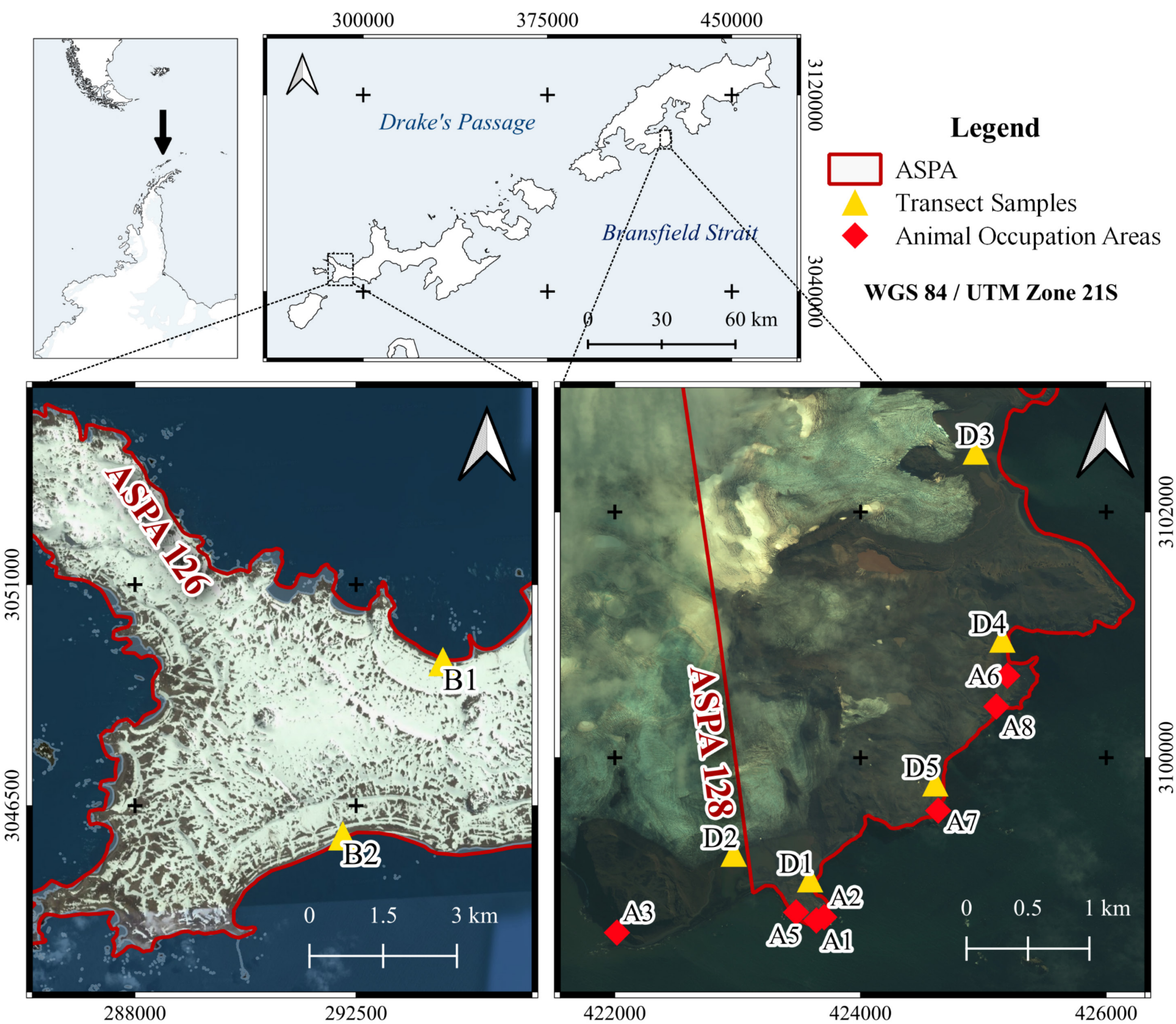

Figure 1. Location of sampling transects in ASPA 126 (left) and 128 (right).

is home to research stations and refugees of different nationalities (Brazil, Poland, Peru, and Ecuador), which are the main anthropic activities in the region.

It has a typical marine climate, with unstable conditions of high atmospheric dynamics (Dąbski et al. 2017, Kejna et al. 2013). Cyclones transport relatively warm and humid air, with strong winds and high precipitation (Bintanja 1995, Ferron et al. 2004). The average atmospheric temperature of the region (series 1982-2002, Comandante Ferraz Antarctic Station) varies from -6.4 ºC in winter to 2.3 ºC in summer (Schaefer et al. 2007), with average annual precipitation (series 1978-1996) of 506 mm (Marsz & Styszynska 2000). ASPA 128 is located on the leeward coast of the island since wind directions are predominantly west, north, northwest, and southeast (Bintanja 1995, Braun et al. 2001). Leeward coasts accumulate smaller amounts of plastic and MPs when compared to windward coasts (Ivar do Sul et al. 2009).

Water flowing through the Bransfield Strait influences ASPA 128. The main currents of Bransfield Strait flow in a northeasterly direction, being influenced mainly by waters from the ACC, in the Drake Passage, surface water from the Weddell Sea, and by the continuation of the deep current of the Gerlache Strait (Morozov 2007, Zhou et al. 2002). A stream of warm and salty water flows below the surface from the ACC to the north of the Bransfield Strait, spreading out near the shores of the South Shetland Islands (Morozov 2007), where King George Island is placed. At a local scale, there is a predominant outflow of water from Admiralty Bay to Bransfield Strait and the superficial circulation of water is dependent on wind directions (Morozov 2007, Pruszak 1980).

The nature of beach sediments in the area is predominantly of volcanic (basalts and andesites), belonging to the Demay Point, Utchaka, and Llano Point formations (Birkenmajer 1980). Holocene and periglacial features such as moraines, talus deposits, and raised beaches, uplifted by the glaciogeoisostatic relief promoted by the melting ice on the island, are common in coastal areas (Dąbski et al. 2017, Francelino et al. 2011, Schaefer et al. 2007). In these coastal areas, a characteristic succession of sediment transport dynamics is identified from the escarpment, passing through talus deposits, that often overly to the beach (Dąbski et al. 2017).

In ASPA 128, the fauna is diverse and comprises birds and mammals, including the chinstrap penguin (*Pygoscelis antarctica*), gentoo penguin (*Pygoscelis papua*), brown skua (*Stercorarius lonnbergi*), elephant seals (*Mirounga leonine*), and Antarctic fur seals (*Arctocephalus gazella*). Areas inhabited by birds and mammals promote intense transfer of carbon and nutrients to the soils, contributing to the formation of ornithogenic soils, which afford greater stability against erosion and favor enrichment by organic matter, allowing the chemical development of soils (Schaefer et al. 2007, Simas et al. 2007). Here, ornithogenic areas generally occur on marine terraces, at backshore zones, and are potential areas for the accumulation of MPs (Moreira et al. 2016).

ASPA 126

ASPA 126 (84.7 km²; 62°34’35” S, 61°13’07” W) is located on the Byers Peninsula, Livingston Island, South Shetlands Archipelago (Figure 1). Livingston Island is, together with King George Island, part of the warmest and wettest regions in Antarctica (Bañón et al. 2013). Climate on Livingston Island is also influenced by intense cyclone formation, with average temperatures ranging from 1.0 °C in summer to -6.6 °C in winter. The mean annual precipitation (Spanish Antarctic Station Juan Carlos I series) is 444.5 mm, with liquid precipitation predominant in summer. Livingston Island has similar atmospheric circulation to King George Island in a Maritime Antarctic context, with low pressure and cyclones from the Antarctic Peninsula and Drake Passage bringing moist ocean air to the southeast coast (Ferron et al. 2004, Bañón et al. 2013). On a local scale, wind speeds in the Byers Peninsula are rarely low, with an average of 26 km h^{-1} and a higher frequency from northeast and southwest directions (Bañón et al. 2013).

The Byers Peninsula is also influenced by water masses flowing through Bransfield Strait to the south and water masses flowing through the Drake Passage to the north, with a predominant west-east flow represented by the ACC (Challenor et al. 1996). The two islands studied here are opposite extremes of the main current that flows in the Bransfield Strait, but ASPA 126, at Livingston Island, is directly influenced by the Drake Passage’s west-east main flow promoted by the ACC (Challenor et al. 1996, Morozov 2007, Zhou et al. 2002).

ASPA 126 represents the largest ice-free area in Maritime Antarctica (60.6 km²), where drainage channels are adapted to the network of volcanic fracturing (López-Martínez et al. 2016, Quesada et al. 2009, Villagran et al. 2013). The landscape results from structural, periglacial and marine dynamic systems, with Holocene beaches and paleo-beaches representing up to 19% of the area (López-Martínez et al. 2016). The lithology is composed of volcaniclastic, sedimentary, and extrusive igneous rocks. Periglacial features such as polygonal soils, raised beaches, and talus deposits are widespread (López-Martínez et al. 2016, Villagran et al. 2013). The presence of drainage channels and the low content of soluble salts in the beach soils suggest the occurrence of significant leaching through the soil profiles, even in soils close to the sea, where the contribution of marine aerosols is more abundant (Navas et al. 2008). Having one of the most complete sets of landscape units in Antarctica, with characteristic biological, hydrological, and geological interactions, the ASPA 126 area is considered a reference site for studies on terrestrial and coastal ecosystems of the South Shetlands Archipelago (Quesada et al. 2009).

MATERIALS AND METHODS

Sampling strategy

Sediments were sampled during the Brazilian Antarctic Operation – OPERANTAR XXXVIII (February 8th – March 1st, 2020). Samples were collected using a stainless-steel spatula which was cleaned with a plastic-free paper towel between sampling procedures to minimize cross-contamination; samples were sealed in aluminum foil before transport.

In ASPA 128, 5 beaches facing the entrance of the Admiralty Bay and the Bransfield Strait were sampled seeking to assess influences of the currents that flow in both areas (Figure 1; Table I). Sampled beaches have a dissipative character and sampling was concentrated in segments of sandy sediments in beaches with a representative presence of pebbles and cobbles (D5 and D3). Sediments were sampled (~ 900 g per site) in transects on the strandlines (foreshore, one or two when available), and raised beaches (backshore; Table I and Figure 2). Strandlines are in the intertidal zone, with greater dynamics of reworking and potential transfer of MPs, while the backshore zone generally acts as a zone of settlement and accumulation of MPs (Turra et al. 2014, Moreira et al. 2016). At least three samples, distanced by ~20 m, were collected in each transect zone at an average depth of 5 cm. Sediment samples (~ 300 g per site) were also collected, in triplicate, in representative areas occupied by Antarctic marine fauna identified by the presence of visible excrements. Composite samples merged individual samples within each transect and were grouped according to beach zone or animal occupation (mammals – *Arctocephalus gazella*, *Mirounga leonine*; or penguins – *Pygoscelis antarctica*).

In ASPA 126, sampling covered a beach facing the Bransfield Strait and another beach facing Drake's Passage, also to assess influences of the currents that flow in both areas (Figure 1). Both beaches are dissipative, and sediments were sampled (~ 900 g per site) in transects on the strandline, with stratified samples at 0-5 cm and 5-15 cm (Table I). Five samples, distanced by ~10 m, were collected at each depth. Composite samples merged individual samples within each transect and grouped according to their depth (0-5 cm and 5-15 cm).

Extraction and analysis of microplastics

At the laboratory, samples were oven-dried at 50 ºC until they reached constant mass. To obtain composite samples (herein called simply as samples), single samples were merged in a glass container and quartered using a stainless-steel spatula on a paper surface inside a fume

Table I. Sampling coordinates and description in ASPA 128 and 126.

Transect ID (Composite sample)	Coordinates of central point	Sampling description
ASPA 128		
D1	21E 423589 3099012	Transect on the foreshore zone over a single strandline (n=5). Points are 15 m apart.
D2 (1), (2)	21E 423033 3099281	Transect on the foreshore zone over the high (1, n=3) and low strandline (2, n=3). Points are 25 m apart.
D3	21E 424886 3102562	Transect on the foreshore zone over a single strandline (n=5). Points are 40 m apart.
D4 (1), (2), (3)	21E 425155 3101011	Transect on the foreshore zone over the high (1, n=3) and low strandline (2, n=3), and on the backshore zone, over the raised beach (3, n=3). Points are 40 m apart.
D5 (1), (2)	21E 424658 3099566	Transect on the foreshore zone over a single strandline (1, n=3), and the backshore zone over the raised beach (2, n=3). Points are 70 m apart.
Ac1	-	Areas occupied by *Mirounga leonina* and *Arctocephalus gazella* (single samples A1, A3, A6, A7)
Ac2	-	Areas occupied by penguins (*Pygoscelis antarctica*) (single samples A2, A5, A8).
ASPA 126		
B1 (1), (2)	20E 601929 3054267	Transect on the foreshore zone over the strandline, on a beach facing the Drake Passage. Points are 10 m apart. Samples collected at depth of 0-5 cm (1, n=5) and 5-15 cm (2, n=5).
B2 (1), (2)	20E 599573 3050927	Transect on the foreshore zone over the strandline, on a beach facing the Bransfield Strait. Points are 10 m apart. Samples collected at depth of 0-5 cm (1, n=5) and 5-15 cm (2, n=5).

hood to minimize air-born contamination. An aliquot of 100 g was taken from dried samples and sieved to isolate particles between 500 µm and 5 mm in size for further analysis (Hidalgo-Ruz et al. 2012).

Density separation and chemical digestion

Sediment samples were then density-separated using a saturated saline solution. In a glass beaker, samples were mixed with 300 mL of a saturated solution of NaCl (density ≈ 1.17 g cm^{-3}). The mixture was stirred with a magnetic stirrer for 20 min, and then left to settle for 2-24 h depending on the silt + clay contents (Figure S1; Table SII). The supernatant was vacuum filtered on a paper filter (Quanty, Brazil, ∅ ≈ 28 µm). This step was repeated two times for all samples.

Particles retained on the paper filter were then rinsed and covered with H_2O_2 30% into a glass beaker for at least 24 h (maximum 240 h) and then vacuum filtered on paper filters (Enders et al. 2020). Biota-rich sediments were additionally digested by adding 0.15 parts of KOH 1.12 kg L^{-1} and 0.15 parts of NaClO 14% of active chlorine to 0.7 parts of filtered distilled water. The solution was added to the glass beaker and the digestion process took place for 5 h, with subsequent filtering of the samples on paper filters. For these samples, the digestion step preceded the density separation step.

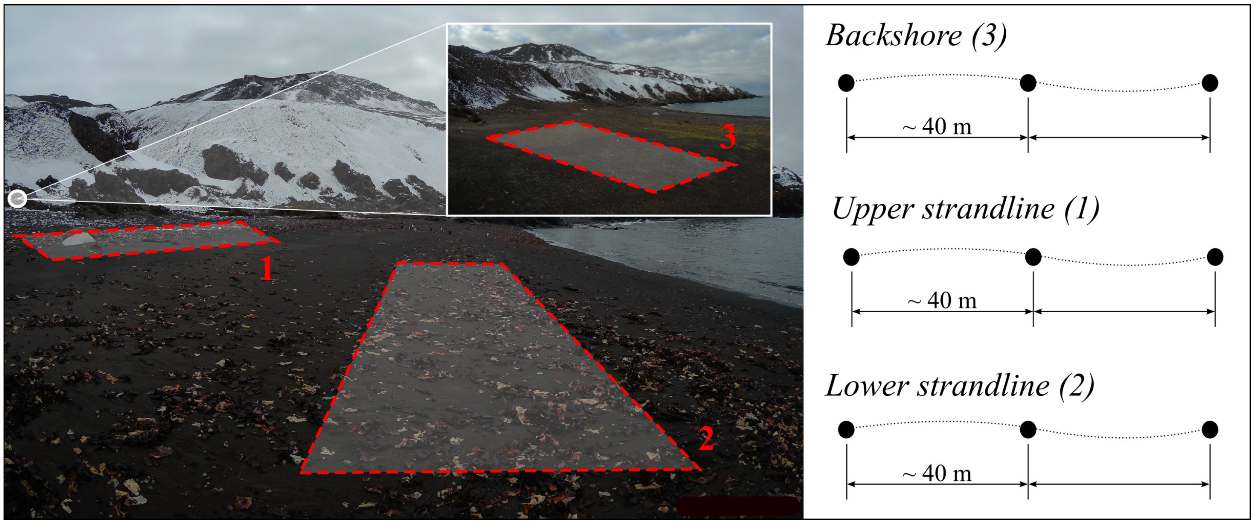

Figure 2. Schematic example of the sampling strategy in transects of the D4 site. Black dots represent sampling points.

Visual analysis: counting and morphological description of MPs

Paper filters were visually analyzed with a ZEISS Stemi 2000-C microscope, equipped with the AxioCam Erc 5s, at magnifications from 0.65x to 5x, for identification, counting, and description of potential MP particles. The following criteria were adopted (Hidalgo-Ruz et al. 2012): no visible organic structures; fibers with a constant thickness along their length; particles with homogeneous and distinguishable colors. The identified MP-like particles were described and classified according to the standardized size and color sorting system (SCS) (Crawford & Quinn 2017).

Polymer identification: micro-Raman analysis

All potential MP particles (n = 91; including fibers, later disregarded) were submitted to qualitative characterization using a micro-Raman inVia® RENISHAW. The spectra were obtained at a 50x magnification, using a 785 nm laser at 0.15 mW on the samples, with an acquisition time of 10 s and 10 accumulations. The spectra acquisition covered a range from 700 to 1800 cm^{-1}, optimal for identifying the main plastic polymers (Anger et al. 2018). When necessary, extended spectra were obtained, covering 200 cm^{-1} to 3200 cm^{-1}. At least three spectra were obtained for each particle at different particle points.

Spectra were then analyzed using Spectragryph-id v1.2.15 software and processed with adaptive baseline correction and peak normalization. Polymers identification was made through Pearson's correlation algorithm, relating the entire spectra, original and the first derivative, with a reference database. Matches with >70% similarity were accepted, while those with 40-70% of similarity were individually examined. It was used the SloPP and SloPP-E (Spectral Library of Plastic Particles and Spectral Library of Plastic Particles Aged in Environment, respectively) reference databases, made available for free use by the Rochman Lab, University of Toronto (Munno et al. 2020).

Contamination control

Contamination control approaches were adopted to reduce cross-contamination risk in laboratory procedures (Enders et al. 2020, Frias et al. 2018, Prata et al. 2021). All sample handling procedures were performed in a fume hood. A cotton coat and nitrile gloves were worn throughout the sample handling procedures.

The samples were stored and handled in glass, paper, or aluminum containers, avoiding contact with plastic surfaces. All glassware was previously cleaned with deionized water previously filtered on paper filters with pores of ~8 µm (Quanty, ∅ ≈ 8 µm). Chemicals were also previously filtered on paper filters (∅ ≈ 8 µm) to be considered MP-free. Inside the fume hood, paper filters were placed in Petri dishes to monitor the airborne deposition of particles whenever samples or reagents were opened to air (atmospheric blanks, BrA). Contamination control in sample handling was evaluated with procedural blanks (BrP), which followed the same processing steps of the environmental samples.

Three BrA and three BrP showed an average of 6.6 (± 1.8) and 4.0 (± 3.0) anthropogenic fibers per sample, respectively. The same fibers were also identified in 14 of the 15 environmental samples (93%), with a mean of 3.1 (± 1.7) fibers per sample. No anthropogenic particles with another shape in the size range of this study were identified in blank samples. Using a conservative approach, fibers were excluded from the final results and only fragments, films and foams are presented here.

Grain size analysis

Mineral particles of the samples were subjected to a grain size analysis, as proposed by Folk & Ward (1957). Aliquots of 100 g of dried and sieved (2 mm; -1.0 φ) bulk samples were taken and sieved in a Ro-Tap machine for 15 minutes. Nine sieves of successive intervals of approximately 0.5 φ (0 φ; 0.5 φ; 1.0 φ; 1.5 φ; 2 φ; 2.25 φ; 3 φ; 3.75 φ; 4.25 φ) were used, and the retained material was weighed. Due to the presence of gravel-sized material (Φ > 2 mm) in all samples, the entire gravel fraction, previously separated, was sieved at successive intervals of 1 φ (-2 φ; -3 φ; -3.75 φ). The data were analyzed using statistical parameters mean, median, sorting (standard deviation), skewness, kurtosis, cumulative and individual frequency curves. The curves and statistical analysis were obtained using SysGran v3.0 software. Results of grain size parameters were analyzed and classified following the proposition by Folk & Ward (1957), summarized in Table SII. Additionally, the mean particle density was determined using the volumetric flask method (Donagemma et al. 2011).

RESULTS

Microplastics in beach sediments from ASPA 128 and 126

This study found large MPs in beach sediments from two terrestrial ASPA in Maritime Antarctica, but in low numbers. A total of three MPs and one anthropogenic particle with unknown synthetic composition were identified in four of 15 (27%) samples, and no MP was identified within samples in animal occupation areas (Table SI - Supplementary Material). The low MP numbers found here impaired any generalization of mean concentration and statistical comparison between sampled habitats. Because of methodological limitations in contamination control, fibers were excluded from the results.

Polymeric compositions of the particles were efficiently confirmed by micro-Raman spectroscopy as a yellow fragment of polypropylene (PP; D4(1) sample, n = 1), a transparent film of polyethylene (PE; D5(2) sample, n = 1), an orange fragment of polyethylene terephthalate (PET; B1(1) sample, n = 1), and, possibly, a white styrene-isoprene copolymer foam (SI/SIS; D2(1), n = 1). The presence of a PET particle was unexpected, due to its density (≈ 1.55 g cm^{-3}) being greater than that of the saline solution used (≈ 1.17 g cm^{-3}), and it was attributed to having been carried by poorly digested large organic particles – present in most of the analyzed filters. Particle's size ranged between 0.5 and 5 mm.

The similarity of the polymers spectra from sampled particles with the database spectra reached 92% (PE), 84% (PET), 70% (PP), and 45% (SI/SIS) for the unconfirmed particle. When closely analyzing spectrum of MP/2/FI/TP/PE (Figure 3a), the prominent peaks of PE can be observed at 1064 cm^{-1}, 1130 cm^{-1}, associated with skeletal vibrations, and at 1296 cm^{-1}, 1418 cm^{-1}, 1442 cm^{-1}, 1459 cm^{-1}, assigned to CH_2 wagging, deformation and bending (Lenz et al. 2015). Spectrum of MMP/0.8/MFR/OR/PET (Figure 3b; B1(1) sample) showed prominent peaks are 1116 cm^{-1} (C(O)-O and C-C bonds), 1177 cm^{-1} (ring in plane C-H bonds, and C-C stretching), 1281 cm^{-1} (C(O)-O stretching), 1453 cm^{-1} (CH_2 and OCH bending), 1615 cm^{-1} (ring mode) and 1730 cm^{-1} (C=O stretching) (Boerio et al. 1976). Peaks near 2960 cm^{-1} and 3081 cm^{-1}, assigned to CH_2 vibrations and CH aromatic bonds, respectively, are reduced and almost imperceptible. The reduction of these peaks is attributed to the UV degradation of PET structures (Rebollar et al. 2014).

MMP/0.5/MFR/YL-BL/PP particle has two colours, and the Raman signal obtained from representative points of each colour resulted in different spectra (Figure 4; D4(1) sample). Both spectra have prominent peaks associated with vibrations of CC, CH_3, and CH_2 bonds of polypropylene (Andreassen, 1999). However, colored pigments can mask the characteristic peaks of polymers (Munno et al. 2020), and it

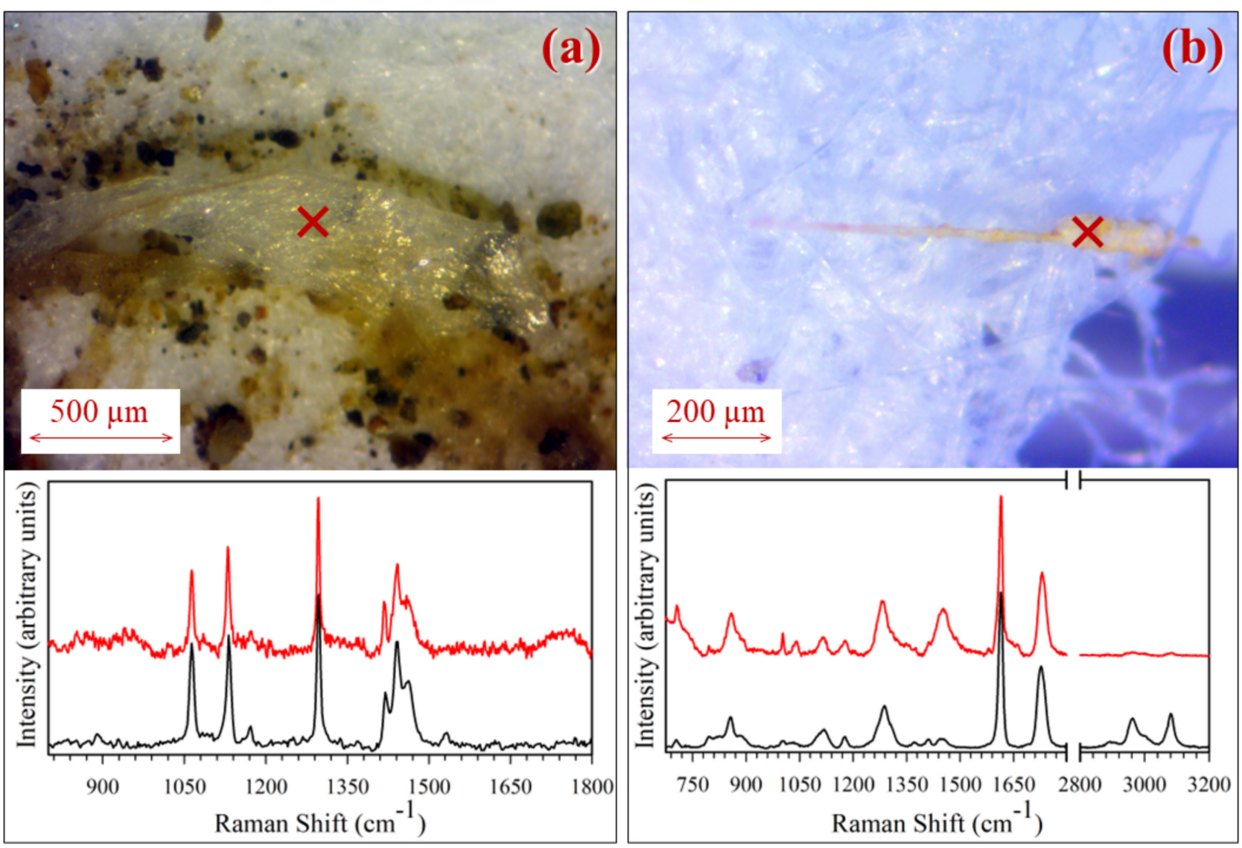

Figure 3. MPs identified in sediment samples with their respective Raman spectra (red lines) and the correlated spectra from the database (black lines). The red X indicates the position of obtaining the spectrum on the particle. (a) MP/2/FI/TP-WT/PE particle, D5(2) sample. (b) MMP/0.8/MFR/OR/PET particle, B1(1) sample.

is likely what is observed here. The spectrum related to blue pigments of the particle corresponds to Phthalocyanine Blue (Figure 4), a dye already observed in a MP particle sampled in subtidal sediments of the Southern Ocean (Van Cauwenberghe et al. 2013).

Despite the MP/5/FM/WT particle being misidentified, it is possible to identify the prominent peaks of polystyrene and polyisoprene (Figure 5a): polyisoprene C=C stretching at 1660 cm^{-1} overlapping the peak at 1600 cm^{-1} assigned with the stretching or bending vibration of the polystyrene aromatic ring; polyisoprene CH_2 deformation at 1440 cm^{-1}; polystyrene CH bending and polyisoprene CH_3 bonds at 1035 cm^{-1}; and C-C skeletal stretching vibration at 1000 cm^{-1} for both polymers (Arjunan et al. 2001, Sears et al. 1981). The SI/SIS copolymers are thermoplastic resins, often used in adhesive, sealing, and elastic materials, and also added to other thermoplastics to improve their physical properties. The thermoplastic nature of this particle was confirmed by applying the unconventional hot needle test (Figure 5b). However, as it was not possible to confirm its polymeric composition, the particle was classified as anthropogenic.

Sediment grain size analysis and sedimentological parameters

Sediment size ranged from granules to coarse sand, with the mean grain size ranging from -1.09 to 0.92 φ (2.13 to 0.53 mm) (Figure 6a) and median from -0.81 to 1.18 φ (1.74 to 0.44 mm). Sorting (1.24 to 2.28 φ) indicated poorly and very poorly sorted sediments (Figure 6a). Negative or very negative skewness was observed in most (73%) samples, indicating a reduction in the tail of fine grains and evidence of the coarse texture of sediments (Table SIII). Kurtosis was the only parameter that showed a high positive correlation (r, Pearson) with the mean and median sediment size of samples (0.80 and 0.79, respectively), suggesting that samples with finer mean grain size (larger means in the phi scale) tend to have a leptokurtic character (Figure 6b).

Samples collected in different beach zones in ASPA 128 do not differ in skewness, kurtosis, mean, and median grain size (Table II). Comparing the surface samples collected in the strandlines of the two ASPA, sorting was the only parameter that presented a statistically significant difference (Mann-Whitney, α = 0.10) (Table II).

Particle density and sorting singularities (Kruskall-Wallis, α = 0.10) between sampled

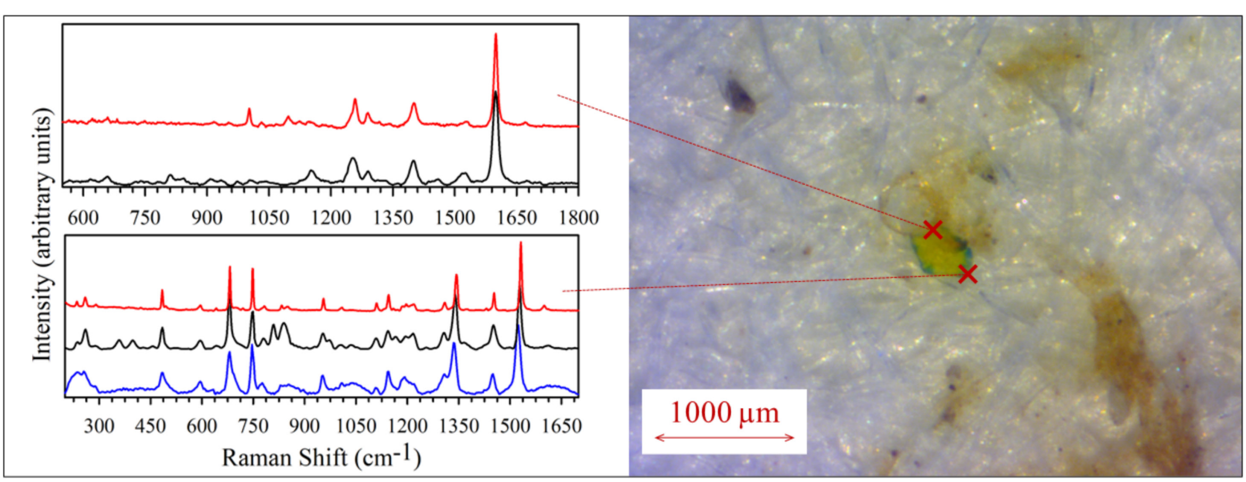

Figure 4. MMP/0.5/MFR/YL-BL/PP particle, D4(1) sample, with respective Raman spectrum (red line) and the correlated spectra from the database (black line). Blue line refers to Phthalocyanine Blue spectrum.

habitats reflected distinct trends in the cumulative frequency curves (Table II; Figures S2 and S3, Supplementary Material). The individual frequency curves of sediment samples collected in the high strandline (Figure 7b) reveal heterogeneous sedimentation, corroborating their poor sorting character (Table II). On the other hand, samples collected in single and lower strandlines, still subject to reworking processes by wave action, are well-sorted and showed a trend close to unimodal in the individual frequency curves (Table II; Figures 6a and 6c). Samples collected on the backshore, over the raised beaches, presented a trend close to bimodal, with a first peak centered at 0 φ and the second peak centered at approximately 3.5 φ (Figure 7d), suggesting that mixed sources supply sediments.

DISCUSSION

This study confirmed the presence of MPs (> 0.5 mm; fibers excluded) in the ASPAs sampled, but there is no evidence of representatively widespread contamination. Indeed, the absence of MPs in most samples does not corroborate some previous studies in the Antarctic ecosystem, when authors reported MP amounts comparable to those found in lower latitudes (Almela & Gonzalez, 2020, Cunningham et al. 2020, Lacerda et al. 2019, Lozoya et al. 2022, Munari et al. 2017, Waller et al. 2017). However, low numbers of MPs were also reported in the Southern Ocean and

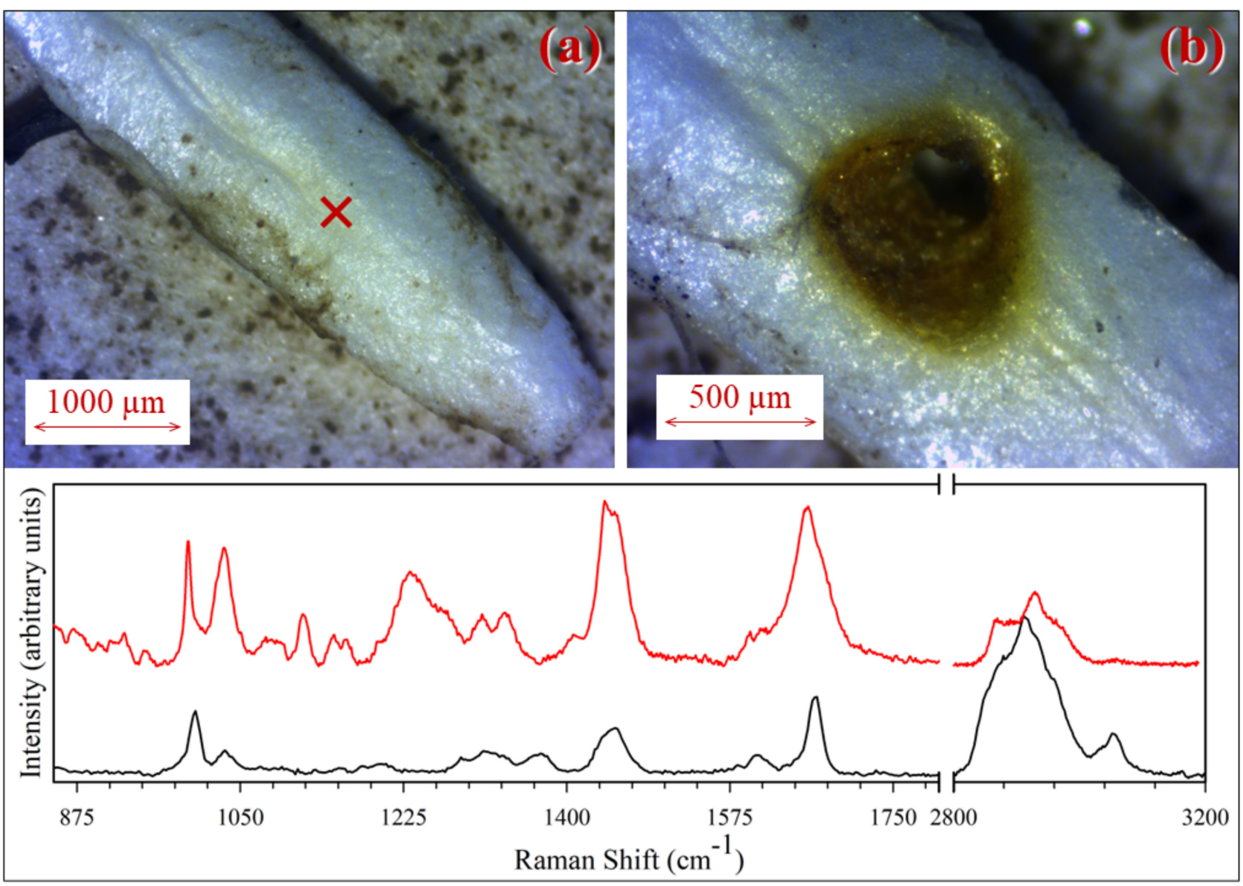

Figure 5. (a) MP/5/FM/WT particle, D2(1) sample, with respective Raman spectrum (red line) and the correlated spectra from the database (black line). (b) Photo of the particle after passing the hot needle test. The red X indicates the position of obtaining the spectrum on the particle.

Antarctic sediments, especially in areas far from human activities (Kuklinski et al. 2019, Reed et al. 2018, Suaria et al. 2020). These remarks suggest that MP contamination in Antarctica is more representative in the vicinity of research stations, where most human activities occur, than on open ocean or isolated beaches, as noted here. For example, half of 60 samples collected in subtidal marine sediments close to the Rothera Antarctic Research Station, Adelaide Island, is contaminated with MP (2 – 5 mm), especially fibers (Reed et al. 2018). The highest amounts were found closer to the research station (0.3 km), while in samples 7 km offshore it was no longer possible to identify MPs (Reed et al. 2018). Discharge from sewage treatment plants, deterioration of infrastructure coatings from the research stations can act as sources of MPs (Reed et al. 2018, Perfetti-Bolaño et al. 2022), and other local sources such as ships and tourism can contribute to this scenario (Lacerda et al. 2019). Even so, in surveys looking for meso (1 – 10 mm) and macroplastic (> 10 mm) debris hotspots on beaches of ASPA 126, 7.9 – 39.5 items km^{-1} were found, highlighting that plastic pollution is actually present in the protected areas (Almela & Gonzalez 2020). Moreover, the smallest amounts of plastic litter were surveyed on the beach sampled in the present study (Almela & Gonzalez 2020) and perhaps higher MP concentrations can be expected on adjacent beaches of ASPA 126.

To date, few studies have evaluated MPs presence Antarctic beach sediments, mainly at Fildes Peninsula (Lozoya et al. 2022, Perfetti-Bolaño et al. 2022). Perfetti-Bolaño et al. (2022) found MPs (319 µm – 1043 µm) – exclusively fibers – in 4 out of 6 sediment samples, with concentrations up to 4 particles 50 mL^{-1}, although only one fiber was sampled in the reference area (ASPA 150, Ardley Island), similar to what we found here. They investigated a single sedimentological parameter and identified an association between fibers occurrence and larger mean grain size (up to ~1 mm) (Perfetti-Bolaño et al. 2022). This is considerably less coarse than most of the sediment sampled in the present study (Figure 6a), and lower MP abundances were found here. On the other hand, Lozoya et al. (2022) found an average of 150.4 particles m^{-2} (1 – 5 mm), with evidence of local and external sources of contamination supported by a degradation

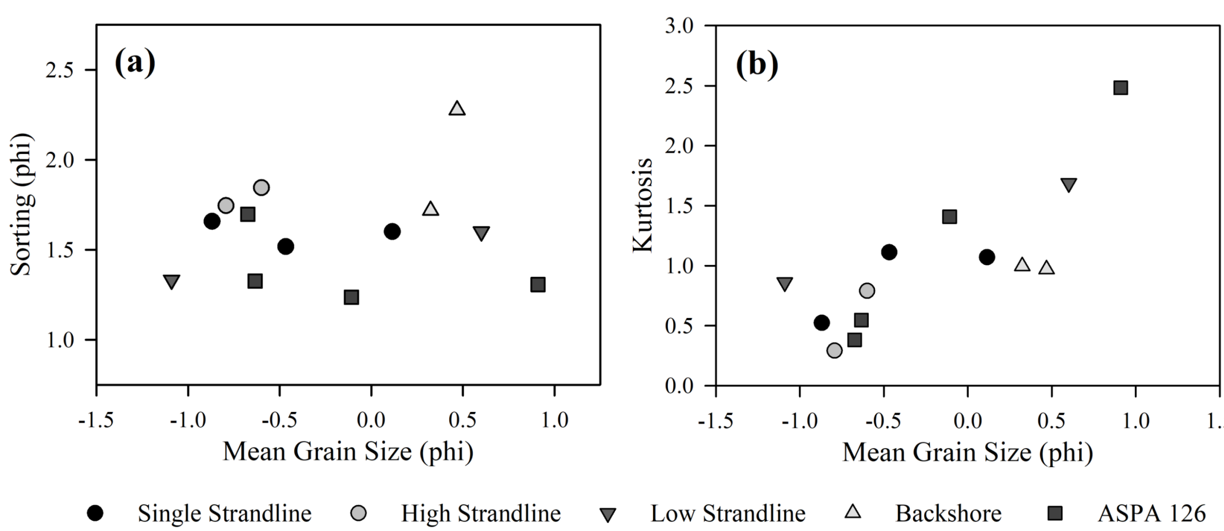

Figure 6. (a) Mean grain size and sorting of all analyzed samples. (b) Mean grain size and kurtosis of all analyzed samples.

index (Carbonyl Index). No characterization of the beach sedimentary environment was given. As the regional environmental context is the same, comparing potential MP distribution with the present study is limited to local factors, such as proximity to contamination sources. Fildes Peninsula is one of the most anthropized areas of Maritime Antarctica, hosting the main airport to access the region (Teniente Rodolfo Marsh Airport), and higher MP concentrations are to be expected than on ASPAs beaches.

The disagreement between results in biota-rich-sediments (Garcia-Garin et al. 2020, Bessa et al. 2019, Fragão et al. 2021, Le Guen et al. 2020) suggested that fibers are the dominant shape of MP contamination found in Antarctic biota. Therefore, sources of MPs in maritime Antarctica are not solved yet. It has already been demonstrated that MPs can cross the ACC barrier through the wave-driven Stokes Drift (Fraser et al. 2018, Onink et al. 2019), and be eventually trapped in the Antarctic maritime ecosystem (Isobe et al. 2017, Lacerda et al. 2019). Fieldwork research also indicate long-distance maritime and atmospheric transport of MP particles (González-Pleiter et al. 2020, Lozoya et al. 2022). Authors also highlight that low-density polymers are associated with long-distance transport, while high-density polymers and resins are more prone to have local sources (Jones-Williams et al. 2020, Lacerda et al. 2019). Low-density (PE, PP) and resin particles were found here, but the low numbers do not allow any conclusions to be drawn about their potential source and distribution patterns.

Despite the low MP numbers having hampered the comparison of their distribution in the different beach environments sampled, MPs are components within sedimentary dynamics (Enders et al. 2019), and a detailed description of environmental factors affecting MP deposition is substantial for beach assessments. Here we

Table II. Sedimentological parameters (mean; standard deviation) of samples collected on different strandlines and the backshore in ASPA 128, and sedimentological parameters (mean; standard deviation) of surface samples collected from strandlines on beaches of ASPAs 128 and 126.

Sampling environment ***Composite samples***	**Mean**	**Median**	**Sorting**	**Skewness**	**Kurtosis**	**Particle density**
	φ	**φ**	**φ**			**g cm^{-3}**
Single strandline *D1, D3, D5(1)*	-0.41$_a$ (0.50)	0.06$_a$ (0.59)	1.59$_b$ (0.07)	-0.31$_a$ (0.31)	0.90$_a$ (0.33)	2.81$_a$ (0.02)
High strandline *D2(1), D4(1)*	-0.70$_a$ (0.14)	-0.12$_a$ (0.51)	1.79$_a$ (0.07)	-0.16$_a$ (0.52)	0.54$_a$ (0.35)	2.63$_{ab}$ (0.10)
Low strandline *D2(2), D4(2)*	-0.24$_a$ (1.20)	0.19$_a$ (1.40)	1.47$_b$ (0.19)	-0.44$_a$ (0.15)	1.27$_a$ (0.58)	2.60$_b$ (0.23)
Backshore *D4(3), D5(2)*	0.40$_a$ (0.10)	0.20$_a$ (0.05)	2.00$_a$ (0.39)	0.15$_a$ (0.07)	0.98$_a$ (0.02)	2.46$_b$ (0.11)
ASPA 128 *D1, D2(1) D2(2), D3, D4(1), D4(2), D5(1)*	-0.41 (0.56)	0.06 (0.66)	1.58* (0.18)	-0.31 (0.29)	0.93 (0.42)	2.69 (0.14)
ASPA 126 *B1(1), B2(1)*	0.40 (0.72)	0.60 (0.77)	1.27* (0.05)	-0.45 (0.15)	1.95 (0.76)	2.80 (0.20)

/ Means with the same letter belong to the same group (Kruskal-Wallis, α = 0.10). Asterisked means represent a significant difference (Mann-Whitney, α = 0.10).

explore sedimentological statistical parameters, used to distinguish depositional environments, to obtain clues that help explain the low numbers of MPs found.

Strandlines are the product of the dynamics of material deposition in recent tidal cycles (Turrell 2018, Pinheiro et al. 2019), and the sampled environments differ in sorting and deposited particle density (Table II). During the tidal rise, the strandline is suspended by wind-wave action and is deposited on the top of the beach into a single strandline, or into upper and lower strandlines as the sea recedes (Turrell 2018). Results here suggested that sediment reworked in the lower strandline during sea retreat is better sorted than that previously deposited in the upper strandline, while single strandline beaches have denser particles deposited (Table II). Thus, coarser and heavier sediment is transported and deposited on the beach, while the finer and lighter material is carried back to the water even when energy decreases on backwash (Martins 1965, Stanica & Ungureanu 2010), which may also occur with MP particles. Furthermore, poorer selection in the upper strandline environment and especially in the backshore environment may be promoted by land-based sedimentary input, which is also suggested by the individual frequency curves (Figure 7b).

Sorting and skewness are generally considered environmentally sensitive factors that reflect the variety of sediment sources and mixing processes, while the mean and median

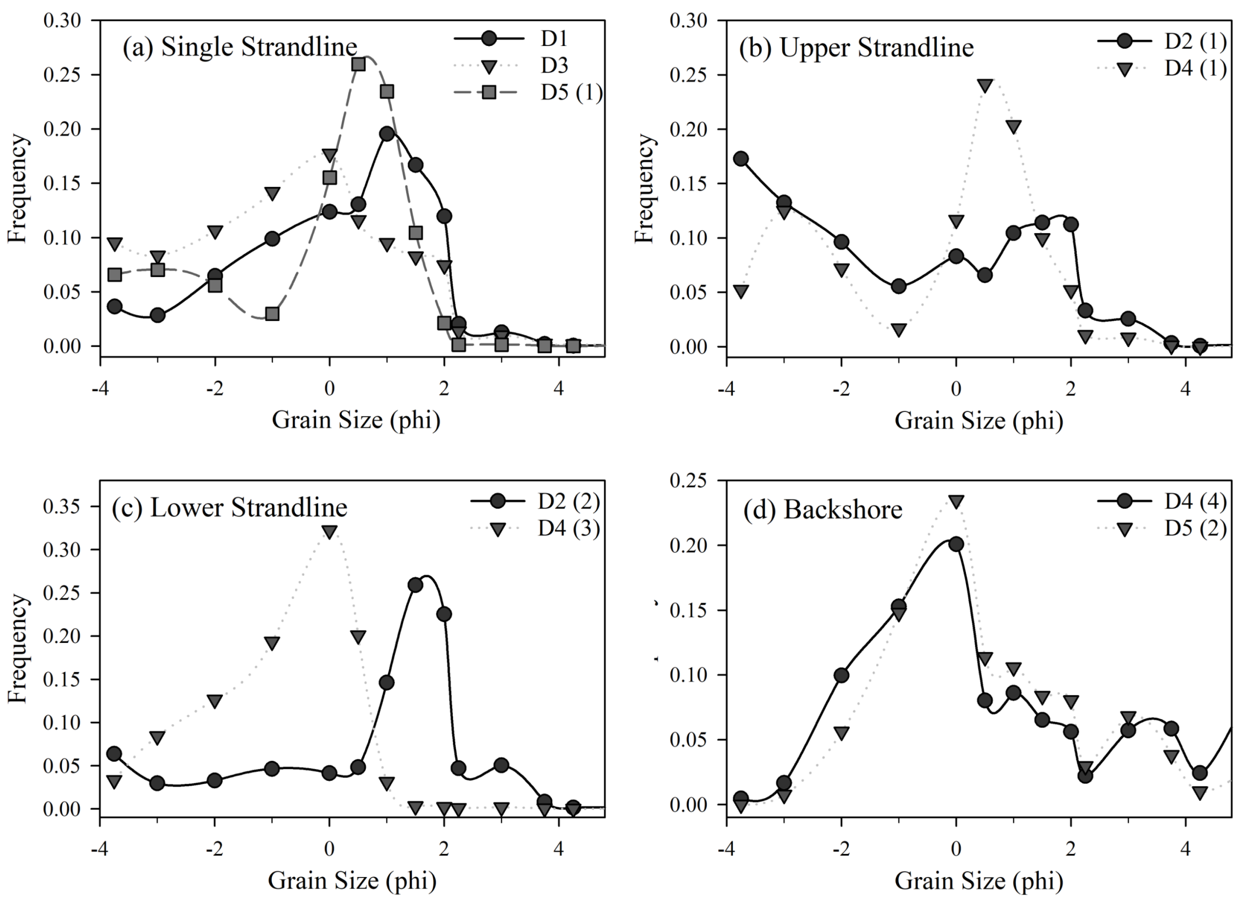

Figure 7. Individual frequency curves for the sampled zones. (a) Single Strandline. (b) Upper Strandline. (c) Lower Strandline. (d) Backshore.

grain size reflect the energy associated with transport mechanisms (Abdulkarim et al. 2015, Edwards 2001). Negative skewness, observed in most samples (73%), is predominant on Holocene beaches and is related to the intensity and duration of the action of a high-energy depositional agent such as wave action, which the input of coarse material can also accentuate to the sedimentary package (Martins 2003). In areas more protected from hydrodynamic action, skewness tends to be positive (Martins 2003), as observed in the backshore samples [D4(3) and D5(2)]. The mean and median grain size of the sediment from the sampled environments did not show significant differences and is predominantly coarse (Table II), which also denotes a high-energy depositional environment. Low-density MPs, such as those found in ASPA 128, are correlated with low-energetic depositional environments that sort fine grains (Enders et al. 2019). So, it is reasonable that MPs were only identified in the most poorly sorted environments at ASPA 128, since in the sampled beaches sorting acts on the predominant coarse grains (Table II) and maybe selective deposition of MPs is less likely.

Even though the sampled environments have significant differences in sorting, all samples are poorly or very poorly sorted (Figure 6a; Table SII). In the sedimentary dynamics of beach environments, the cyclic process of reworking by wave action is expected to provide constant transport energy and, consequently, promote the efficient sorting of sediment grains (Stanica & Ungureanu 2010). However, climate at the Maritime Antarctica region is greatly influenced by successive cyclone systems and turbulent ocean currents with high kinetic energy (Chereskin et al. 2009, Ferron et al. 2004), and the beach environments are often characterized as stormy beaches (Fretwell et al. 2010, do Vale Lopes et al. 2022). Even with the beach environments subject to selective wave action, the susceptibility of these areas to stormy events may contribute to the formation of a coarse and poorly sorted sedimentary package on beaches of ASPA 126 and 128.

Erosion promoted by stormy events also influences the removal of MPs from beach surface sediments while fair weather conditions contribute to their re-deposition on beaches (Chubarenko & Stepanova 2017). Smaller and less dense particles settle in low-energy environments, and, despite it is not yet clear (Perfetti-Bolaño et al. 2022), the behavior of MPs is expected to be similar (Harris 2020). For example, beaches protected by seawalls or beachrocks subject to less energetic dynamics tend to have higher concentrations of MPs (Pinheiro et al. 2019), and there is a positive and significant correlation between the abundance of high-density MPs with fine sand and medium silt contents in relatively low-energetic depositional environments (Enders et al. 2019). Moreover, finer-grain sediments can entrap MPs more efficiently than coarse-grained sediments (Mendes et al. 2021). Therefore, low numbers of MPs in this study suggest that the sedimentary dynamics of the beach environment from ASPAs 128 and 126, which favors the formation of a coarse and poorly sorted sedimentary package, impair the widespread accumulation of MPs (> 0.5 mm; fibers excluded).

METHODS REMARKS AND LIMITATIONS

Although the low numbers of MPs may reflect a lower input in the ASPA areas, reinforced by a beach sedimentary environment that does not favor the accumulation of MPs, it is important to emphasize that differences in the used methods make direct comparisons difficult. For example, the transect sampling approach used here was fully exploratory, seeking to identify distribution patterns of MP contamination on different beach strandlines. On the other hand, most studies that reported high MPs concentrations in the Antarctic environment used a judgmental sampling strategy approach, with subjective sampling points selections based on previous information about the area (e.g. proximity to polluting sources, visual inspection) (Lozoya et al. 2022, Munari et al. 2017, Perfetti-Bolaño et al. 2022, Reed et al. 2018). In addition, comparisons between studies may be hampered by the still lack of standardization in reported units. Lozoya et al. (2022) reported 234.4 ± 166 particles m^{-2} in beach sediments from Fildes Peninsula, which if expressed in particles kg^{-1} the values would be comparable to those reported here, although only one particle was identified in each 100 g aliquot.

It is also important to clarify that this study probably underestimates MPs abundance, for three main reasons. First, fibers are the most frequently reported morphology in environmental sediment samples (Van Cauwenberghe et al. 2015), even in polar environments (Tirelli et al. 2020), and were not considered here. Second, small MPs (< 0.5 mm) tend to be more abundant in the environment (Prata et al. 2021), and perhaps larger numbers can be found by lowering the detection size limit. Finally, the using of saline NaCl solution (d ≈ 1.17 g cm^{-3}) may be inefficient for separating of high-density polymers (e.g. PVC and PET). Even though, MP fragments and films have already been identified in large amounts in assessments in the Southern Ocean (Suaria et al. 2020, Lacerda et al. 2019), and represent a potential ecological risk due to the interaction with the Antarctic biota (Bergami et al. 2020, Bessa et al. 2019, Fragão et al. 2021).

CONCLUSIONS AND RECOMMENDATIONS

The present study shows low amounts of large MP particles (0.5 – 5 mm; fibers excluded) in sediment samples from beaches at ASPAs 128 and 126, with a maximum abundance of 1 MP per sample. In most samples (73%), MP contamination was undetectable by the analytical procedure adopted here. Low MP numbers impaired statistical comparisons between amounts and characteristics of MPs sampled in different habitats, and the absence of small MP particles (< 0.5 mm) and fibers cannot be confirmed, as it is subject for another study. MP contamination in Maritime Antarctica seems to be largely heterogeneous. Therefore, only complete characterization of sedimentary environments and processes affecting MP migration, as well as systematization of methods applied to MP studies, can improve current knowledge on plastic distribution patterns. Future studies focused on mammal and bird excrements should evaluate fiber content as evidence of MP contamination.

The sampled environments presented different sedimentological parameters, indicating these areas are subject to different sedimentary dynamics. However, the sediment is predominantly coarse and poorly sorted, and their high-energy dynamics may explain the inexpressive amounts of MPs reported here. Exploring sedimentological approaches is encouraged in future research with MPs in Antarctica.

The Antarctic Treaty has norms to regulate and manage solid waste and liquid effluents, but an increasing human pressure highlights the need for more restricted rules by research stations, refugees, tourists and ships that transit in the Antarctic environment. Development of specific and periodic monitoring strategies is also encouraged, and the MP-scientific community has the challenge to indicate which methods to sample and identify MP in small scales are better to be adopted in the Antarctic continent.

Acknowledgments

The present work was carried out with the support of the Coordenação de Aperfeiçoamento de Pessoal de Nível Superior (CAPES, Brazil) – Financing Code 001. This study was conducted within activities of project PERMACLIMA/TERRANTAR, financed by Conselho Nacional Desenvolvimento Científico e Tecnológico (CNPq) of the Brazilian Minitry of Science, Technology, Innovation and communication – MCTIC, under the scope of Brazilian Antarctic Program (PROANTAR). The authors thank the support of the Brazilian Ministries of Science, Technology and Innovation (MCTI), Environment (MMA) and Inter-Ministry Commission for Sea Resources (CIRM). We also thank F. Menges for providing the Spectragryph-id v1.2.15 license.

REFERENCES

ABDULKARIM R, AKINNIGBAGBE E, IMO D, IMHANSOLOEVA M, ANIEBONE V, IBITOLA M, FALEYE B, SHONDE O & APPIA Y. 2015. Grain size analysis of beach sediment along the barrier bar lagoon coastal system, Lagos, Nigeria; its implication on coastal erosion. Glob J Geo Sci 12(1): 31.

ABSHER TM, FERREIRA SL, KERN Y, FERREIRA AL, CHRISTO SW & ANDO RA. 2019. Incidence and identification of microfibers in ocean waters in Admiralty Bay, Antarctica. Environ Sci Pollut R 26(1): 292-298.

AJITH N, ARUMUGAM S, PARTHASARATHY S, MANUPOORI S & JANAKIRAMAN S. 2020. Global distribution of microplastics and its impact on marine environment—a review. Environ Sci Pollut R 27(21): 25970-25986.

ALMELA P & GONZALEZ S. 2020. Are Antarctic Specially Protected Areas safe from plastic pollution? A survey of plastic litter at Byers Peninsula, Livingston Island, Antarctica. Adv Polar Sci 31(4): 284-290.

ANDREASSEN E. 1999. Infrared and Raman spectroscopy of polypropylene In: Karger-Kocsis J (Ed), Polypropylene. Polymer Science and Technology Series, vol 2. Springer, Dordrecht p. 320-328.

ANGER PM, VON DER ESCH E, BAUMANN T, ELSNER M, NIESSNER R & IVLEVA NP. 2018. Raman microspectroscopy as a tool for microplastic particle analysis. Trac-Trend Anal Chem 109: 214-226.

ARJUNAN V, SUBRAMANIAN S & MOHAN S. 2001. Fourier transform infrared and Raman spectral analysis of trans-1,4-polyisoprene. Spectrochim Acta A 57(13): 2547-2554.

ATCM - ANTARTIC TREATY CONSULTATIVE MEETING. 2014. Management Plan for Antarctic Specially Protected Area No 128 Western Shore of Admiralty Bay, King George Island, South Shetlands Island.

ATCM - ANTARTIC TREATY CONSULTATIVE MEETING. 2016. Management Plan for Antarctic Specially Protected Area No 126 Byers Peninsula, Livingston Island, South Shetland Islands.

BAÑÓN M, JUSTEL A, VELÁZQUEZ D & QUESADA A. 2013. Regional weather survey on Byers Peninsula, Livingston Island, South Shetland Islands, Antarctica. Antarct Sci 25(2): 146-156.

BERGAMI E, ROTA E, CARUSO T, BIRARDA G, VACCARI L & CORSI I. 2020. Plastics everywhere: first evidence of polystyrene fragments inside the common Antarctic collembolan Cryptopygus antarcticus. Biol Lett 16(6).

BESSA F, RATCLIFFE N, OTERO V, SOBRAL P, MARQUES JC, WALUDA CM, TRATHAN PN & XAVIER JC. 2019. Microplastics in gentoo penguins from the Antarctic region. Sci Rep-UK 9(1): 1-7.

BINTANJA R. 1995. The Local Surface Energy Balance of the Ecology Glacier, King George Island, Antarctica: Measurements and modelling. Antarct Sci 7(3): 315-325.

BIRKENMAJER K. 1980. Geology of Admiralty Bay, King George Island (South Shetland Islands) — An outline. Pol Polar Res 1(1): 29-54.

BOERIO FJ, BAHL SK & MCGRAW GE. 1976. Vibrational analysis of polyethylene terephthalate and its deuterated derivatives. J Polym Sci Pol Phys 14(6): 1029-1046.

BRAUN M, SAURER H, VOGT S, SIMÕES JC & GOßMANN H. 2001. The influence of large-scale atmospheric circulation on the surface energy balance of the King George Island ice cap. Int J Climatol 21(1): 21-36.

CAI L, WANG J, PENG J, WU Z & TAN X. 2018. Observation of the degradation of three types of plastic pellets exposed to UV irradiation in three different environments. Sci Total Environ 628-629: 740-747.

CARUSO G, BERGAMI E, SINGH N & CORSI I. 2022. Plastic occurrence, sources, and impacts in Antarctic environment and biota. Water Biol Secur 1(2): 100034.

COMMITTEE OF ENVIRONMENTAL PROTECTION. 1991a. Annex V to the Protocol on Environmental Protection to the Antartic Treaty - Area Protection and Management.

COMMITTEE OF ENVIRONMENTAL PROTECTION. 1991b. Protocol on Environmental Protection to the Antartic Treaty.

CHALLENOR PG, READ JF, POLLARD RT & TOKMAKIAN RT. 1996. Measuring Surface Currents in Drake Passage from Altimetry and Hydrography. J Phys Oceanogr 26(12): 2748-2759.

CHERESKIN TK, DONOHUE KA, WATTS DR, TRACEY KL, FIRING YL & CUTTING AL. 2009. Strong bottom currents and cyclogenesis in Drake Passage. Geophys Res Lett 36(23): 1-5.

CHUBARENKO I & STEPANOVA N. 2017. Microplastics in sea coastal zone: Lessons learned from the Baltic amber. Environ Pollut 224: 243-254.

CINCINELLI A, SCOPETANI C, CHELAZZI D, LOMBARDINI E, MARTELLINI T, KATSOYIANNIS A, FOSSI MC & CORSOLINI S. 2017. Microplastic in the surface waters of the Ross Sea (Antarctica): Occurrence, distribution and characterization by FTIR. Chemosphere 175: 391-400.

CRAWFORD CB & QUINN B. 2017. Microplastic Pollutants. Elsevier Science, 315 p.

CUNNINGHAM EM, EHLERS SM, DICK JT, SIGWART JD, LINSE K, DICK JJ & KIRIAKOULAKIS K. 2020. High abundances of microplastic pollution in deep-sea sediments: evidence from Antarctica and the Southern Ocean. Environ Sci Technol 54(21): 13661-13671.

DĄBSKI M, ZMARZ A, PABJANEK P, KORCZAK-ABSHIRE M, KARSZNIA I & CHWEDORZEWSKA KJ. 2017. UAV-based detection and spatial analyses of periglacial landforms on Demay Point (King George Island, South Shetland Islands, Antarctica). Geomorphology 290: 29-38.

DONAGEMMA GK, CAMPOS DVB, CALDERANO SB, TEIXEIRA WG & VIANA JHM. 2011. Manual de Métodos de Análise de Solo. Embrapa, 230 p.

DO VALE LOPES D, SOARES DE OLIVEIRA F, PEREIRA TTC & SCHAEFER CEGR. 2022. Pedogeomorphology and weathering at Snow Island, Maritime Antarctica. Catena 217: 106515.

EDWARDS AC. 2001. Grain size and sorting in modern beach sands. J Coastal Res 17(1): 38-52.

ENDERS K ET AL. 2019. Tracing microplastics in aquatic environments based on sediment analogies. Sci Rep-UK 9(1): 1-15.

ENDERS K, LENZ R, IVAR DO SUL JA, TAGG AS & LABRENZ M. 2020. When every particle matters: A QuEChERS approach to extract microplastics from environmental samples. MethodsX 7: 100784.

FERRON FA, SIMÕES JC, AQUINO FE & SETZER AW. 2004. Air temperature time series for King George Island, Antarctica. Pesqui Antart Bras 4: 155-169.

FOLK RL. 1966. A Review of Grain-Size Parameters. Sedimentology 6(2): 73-93.

FOLK RL & WARD WC. 1957. Brazos River bar [Texas]; a study in the significance of grain size parameters. J Sediment Res 27(1): 3-26.

FRAGÃO J, BESSA F, OTERO V, BARBOSA A, SOBRAL P, WALUDA CM, GUÍMARO HR & XAVIER JC. 2021. Microplastics and other anthropogenic particles in Antarctica: Using penguins as biological samplers. Sci Total Environ 788: 147698.

FRANCELINO MR, SCHAEFER CEGR, SIMAS FNB, FILHO EIF, DE SOUZA JJLL & DA COSTA LM. 2011. Geomorphology and soils distribution under paraglacial conditions in an ice-free area of Admiralty Bay, King George Island, Antarctica. Catena 85(3): 194-204.

FRASER CI ET Al. 2018. Antarctica's ecological isolation will be broken by storm-driven dispersal and warming. Nat Clim Change 8(8): 704-708.

FRETWELL PT, HODGSON DA, WATCHAM EP, BENTLEY MJ & ROBERTS SJ. 2010. Holocene isostatic uplift of the South Shetland Islands, Antarctic Peninsula, modelled from raised beaches. Quat Sci Rev 29: 1880-1893.

FRIAS J ET AL. 2018. Standardised protocol for monitoring microplastics in sediments. JPI-Oceans BASEMAN Project, May, 33.

GARCIA-GARIN O, GARCÍA-CUEVAS I, DRAGO M, RITA D, PARGA M, GAZO M & CARDONA L. 2020. No evidence of microplastics in Antarctic fur seal scats from a hotspot of human activity in Western Antarctica. Sci Total Environ 737: 140210.

GONZÁLEZ-PLEITER M, EDO C, VELÁZQUEZ D, CASERO-CHAMORRO MC, LEGANÉS F, QUESADA A, FERNÁNDEZ-PIÑAS F & ROSAL R. 2020. First detection of microplastics in the freshwater of an Antarctic Specially Protected Area. Mar Pollut Bull 161: 1-6.

HARRIS PT. 2020. The fate of microplastic in marine sedimentary environments: A review and synthesis. Mar Pollut Bull 158: 111398.

HIDALGO-RUZ V, GUTOW L, THOMPSON RC & THIEL M. 2012. Microplastics in the marine environment: A review of the methods used for identification and quantification. Environ Sci Technol 46(6): 3060-3075.

ISOBE A, UCHIYAMA-MATSUMOTO K, UCHIDA K & TOKAI T. 2017. Microplastics in the Southern Ocean. Mar Pollut Bull 114(1): 623-626.

IVAR DO SUL JA, SPENGLER Â & COSTA MF. 2009. Here, there and everywhere. Small plastic fragments and pellets on beaches of Fernando de Noronha (Equatorial Western Atlantic). Mar Pollut Bull 58(8): 1236-1238.

JONES-WILLIAMS K, GALLOWAY T, COLE M, STOWASSER G, WALUDA C & MANNO C. 2020. Close encounters-microplastic availability to pelagic amphipods in sub-antarctic and antarctic surface waters. Environ Int 140: 105792.

KEJNA, M, ARAZNY A & SOBOTA I. 2013. Climatic change on King George Island (West Antarctica) in the years 1948-2011. Pol Polar Res 34(2): 213-235.

KELLY A, LANNUZEL D, RODEMANN T, MEINERS KM & AUMAN HJ. 2020. Microplastic contamination in east Antarctic sea ice. Mar Pollut Bull 154(March): 111130.

KUKLINSKI P, WICIKOWSKI L, KOPER M, GRALA T, LENIEC-KOPER H, BARASIŃSKI M, TALAR M, KAMIŃSKI I, KIBART R & MAŁECKI W. 2019. Offshore surface waters of Antarctica are free of microplastics, as revealed by a circum-Antarctic study. Mar Pollut Bull 149: 110573.

LACERDA ALDF, RODRIGUES LS, VAN SEBILLE E, RODRIGUES FL, RIBEIRO L, SECCHI ER, KESSLER F & PROIETTI MC. 2019. Plastics in sea surface waters around the Antarctic Peninsula. Sci Rep-UK, 9(1): 1-12.

LE GUEN C, SUARIA G, SHERLEY RB, RYAN PG, ALIANI S, BOEHME L & BRIERLEY AS. 2020. Microplastic study reveals the presence of natural and synthetic fibres in the diet of King Penguins (Aptenodytes patagonicus) foraging from South Georgia. Environ Int 134: 105303.

LEBRETON L, EGGER M & SLAT B. 2019. A global mass budget for positively buoyant macroplastic debris in the ocean. Sci Rep-UK 9(1): 1-10.

LENZ R, ENDERS K, STEDMON, CA, MACKENZIE DMA & NIELSEN TG. 2015. A critical assessment of visual identification of marine microplastic using Raman spectroscopy for analysis improvement. Mar Pollut Bull 100(1): 82-91.

LÓPEZ-MARTÍNEZ J, SCHMID T, SERRANO E, MINK S, NIETO A & GUILLASO S. 2016. Geomorphology and surface landforms distribution in selected ice-free areas in the south Shetland Islands, northern Antarctic Peninsula region. Cuad Investig Geogr 42(2): 435-455.

LÓPEZ-MARTÍNEZ J, SERRANO E, SCHMID T, MINK S & LINÉS C. 2012. Periglacial processes and landforms in the South Shetland Islands (northern Antarctic Peninsula region). Geomorphology 155-156: 62-79.

LOZOYA JP, RODRÍGUEZ M, AZCUNE G, LACEROT G, PÉREZ-PARADA A, LENZI J, ROSSI F & TEIXEIRA DE MELLO F. 2022. Stranded Pellets in Fildes Peninsula (King George Island, Antarctica): New Evidence of Southern Ocean Connectivity. SSRN Electronic J: 119519.

MENDES A, GOLDEN N, BERMEJO R & MORRISON L. 2021. Distribution and abundance of microplastics in coastal sediments depends on grain size and distance from sources. Mar Pollut Bull 172: 112802.

MARTINS LR. 1965. Significance of skewness and kurtosis in environmental interpretation. J Sediment Res 35(3): 768-770.

MARTINS LR. 2003. Recent sediments and grain-size analysis. Gravel 1: 90-105.

MARSZ AA & STYSZYNSKA A. 2000. The main features of the climate region the Polish Antarctic Station H. Arctowski (West Antarctica, South Shetland Islands, King George Island). Wyższa Szkoła Morska, Gdynia, 264 p.

MOREIRA FT, PRANTONI AL, MARTINI B, DE ABREU MA, STOIEV SB & TURRA A. 2016. Small-scale temporal and spatial variability in the abundance of plastic pellets on sandy beaches: Methodological considerations for estimating the input of microplastics. Mar Pollut Bull 102(1): 114-121.

MOROZOV EG. 2007. Currents in Bransfield Strait. Dokl Earth Sci 415(2): 984-986.

MUNARI C, INFANTINI V, SCOPONI M, RASTELLI E, CORINALDESI C & MISTRI M. 2017. Microplastics in the sediments of Terra Nova Bay (Ross Sea, Antarctica). Mar Pollut Bull 122(1-2): 161-165.

MUNNO K, DE FROND H, O'DONNELL B & ROCHMAN CM. 2020. Increasing the Accessibility for Characterizing Microplastics: Introducing New Application-Based and Spectral Libraries of Plastic Particles (SLoPP and SLoPP-E). Anal Chem 92(3): 2443-2451.

NAVAS A, LÓPEZ-MARTÍNEZ J, CASAS J, MACHÍN J, DURÁN JJ, SERRANO E, CUCHI JA & MINK S. 2008. Soil characteristics on varying lithological substrates in the South Shetland Islands, maritime Antarctica. Geoderma 144(1-2): 123-139.

ONINK V, WICHMANN D, DELANDMETER P & VAN SEBILLE E. 2019. The Role of Ekman Currents, Geostrophy, and Stokes Drift in the Accumulation of Floating Microplastic. J Geophys Res-Oceans 124(3): 1474-1490.

PERFETTI-BOLAÑO A, ARANEDA A, MUÑOZ K & BARRA RO. 2022. Occurrence and Distribution of Microplastics in Soils and Intertidal Sediments at Fildes Bay, Maritime Antarctica. Front Mar Sci 8.

PINHEIRO LM, MONTEIRO RCP, IVAR DO SUL JA & COSTA MF. 2019. Do beachrocks affect microplastic deposition on the strandline of sandy beaches? Mar Pollut Bull 141: 569-572.

PRATA JC, REIS V, DA COSTA JP, MOUNEYRAC C, DUARTE AC & ROCHA-SANTOS T. 2021. Contamination issues as a challenge in quality control and quality assurance in microplastics analytics. J Hazard Mater 403.

PRUSZAK Z. 1980. Currents circulation in the waters of Admiralty Bay (region of Arctowski Station on King George Island). Pol Polar Res 1(1): 55-74.

QUESADA A, CAMACHO A, ROCHERA C & VELÁZQUEZ D. 2009. Byers Peninsula: A reference site for coastal, terrestrial and limnetic ecosystem studies in maritime Antarctica. Polar Sci 3(3): 181-187.

REBOLLAR E, PÉREZ S, HERNÁNDEZ M, DOMINGO C, MARTÍN M, EZQUERRA TA, GARCÍA-RUIZ JP & CASTILLEJO M. 2014. Physicochemical modifications accompanying UV laser induced surface structures on poly(ethylene terephthalate) and their effect on adhesion of mesenchymal cells. Phys Chem Chem Phys 16(33): 17551-17559.

REED S, CLARK M, THOMPSON R & HUGHES KA. 2018. Microplastics in marine sediments near Rothera Research Station, Antarctica. Mar Pollut Bull 133.

SCHAEFER CEGR, ALBUQUERQUE MA, CALIJURI ML, FERNANDES FILHO EI, FRANCELINO MR, RAYMOND C, SANTANA RM & SIMAS FNB. 2007. Geoenvironments from the vicinity of Arctowski Station, Admiralty Bay, King George Island, Antarctica; vulnerability and valuation assessment. Open-File Report 1047 - US Geological Survey, Short Research Paper 015.

SEARS WM, HUNT JL & STEVENS JR. 1981. Raman scattering from polymerizing styrene. I. Vibrational mode analysis. J Chem Phys 75(4): 1589-1598.

SFRISO AA, TOMIO Y, ROSSO B, GAMBARO A, SFRISO A, CORAMI F, RASTELLI E, CORINALDESI C, MISTRI M & MUNARI C. 2020. Microplastic accumulation in benthic invertebrates in Terra Nova Bay (Ross Sea, Antarctica). Environ Int 137: 105587.

SIMAS FNB, SCHAEFER CEGR, MELO VF, ALBUQUERQUE-FILHO MR, MICHEL RFM, PEREIRA VV, GOMES MRM & DA COSTA LM. 2007. Ornithogenic cryosols from Maritime Antarctica: Phosphatization as a soil forming process. Geoderma 138(3-4): 191-203.

STANICA A & UNGUREANU V. 2010. Understanding coastal morphology and sedimentology. Terre et Environnement 88(1992): 105-111.

SUARIA G, PEROLD V, LEE JR, LEBOUARD F, ALIANI S & RYAN PG. 2020. Floating macro- and microplastics around the Southern Ocean: Results from the Antarctic Circumnavigation Expedition. Environ Int 136(January): 105494.

TIRELLI V, SUARIA G & LUSHER AL. 2020. Microplastics in Polar Samples. In Handbook of Microplastics in the Environment (p. 1-42). Springer International Publishing.

TURRA A, MANZANO AB, DIAS RJS, MAHIQUES MM, BARBOSA L, BALTHAZAR-SILVA D & MOREIRA FT. 2014. Three-dimensional distribution of plastic pellets in sandy beaches: shifting paradigms. Sci Rep 4: 4435.

TURRELL WR. 2018. A simple model of wind-blown tidal strandlines: How marine litter is deposited on a mid-latitude, macro-tidal shelf sea beach. Mar Pollut Bull 137: 315-330.

VAN CAUWENBERGHE L, DEVRIESE L, GALGANI F, ROBBENS J & JANSSEN CR. 2015. Microplastics in sediments: a review of techniques, occurrence and effects. Mar Environ Res 111: 5-17.

VAN CAUWENBERGHE L, VANREUSEL A, MEES J & JANSSEN CR. 2013. Microplastic pollution in deep-sea sediments. Environ Pollut 182: 495-499.

VAN FRANEKER JA & BELL PJ. 1988. Plastic ingestion by petrels breeding in Antarctica. Mar Pollut Bull 19(12): 672-674.

VIANELLO A, BOLDRIN A, GUERRIERO P, MOSCHINO V, RELLA R, STURARO A & DA ROS L. 2013. Microplastic particles in sediments of Lagoon of Venice, Italy: First observations on occurrence, spatial patterns and identification. Estuar Coast Shelf S 130: 54-61.

VILLAGRAN XS, SCHAEFER CEGR & LIGOUIS B. 2013. Living in the cold: Geoarchaeology of sealing sites from Byers Peninsula (Livingston Island, Antarctica). Quatern Int 315: 184-199.

WALLER CL, GRIFFITHS HJ, WALUDA CM, THORPE SE, LOAIZA I, MORENO B, PACHERRES CO & HUGHES KA. 2017. Microplastics in the Antarctic marine system: An emerging area of research. Sci Total Environ 598: 220-227.

ZALASIEWICZ J ET AL. 2016. The geological cycle of plastics and their use as a stratigraphic indicator of the Anthropocene. Anthropocene 13: 4-17.

ZHOU M, NIILER PP & HU JH. 2002. Surface currents in the Bransfield and Gerlache Straits, Antarctica. Deep-Sea Res Pt I 49(2): 267-280.

SUPPLEMENTARY MATERIAL

Figure S1-S3.
Table SI-SIII.

How to cite
MIRANDA CO, SCHAEFER CEGR, SOUZA JJLL, GUIMARÃES LM, MAIA PVS & IVAR DO SUL JA. 2023. Low numbers of large microplastics on environmentally-protected Antarctic beaches reveals no widespread contamination: insights into beach sedimentary dynamics. An Acad Bras Cienc 95: e20230283. DOI 10.1590/0001-3765202320230283.

Manuscript received on March 14, 2023;
accepted for publication on October 7, 2023

CAIK O. DE MIRANDA[1]
https://orcid.org/0000-0002-3510-2678

CARLOS ERNESTO G.R. SCHAEFER[1]
https://orcid.org/0000-0001-7060-1598

JOSÉ JOÃO L.L. DE SOUZA[1]
https://orcid.org/0000-0003-4670-6626

LUCIANO M. GUIMARÃES[2]
https://orcid.org/0000-0001-9656-2996

PAULO VICTOR S. MAIA[2]
https://orcid.org/0000-0002-1767-1375

JULIANA A. IVAR DO SUL[3]
https://orcid.org/0000-0003-0851-3559

[1]Universidade Federal de Viçosa, Departamento de Solos, Edifício Sylvio Starling Brandão, Av. Peter Henry Rolfs, s/n, Campus Universitário, 36570-900 Viçosa, MG, Brazil

[2]Universidade Federal de Viçosa, Departamento de Física, Centro de Ciências Exatas, Av. Peter Henry Rolfs, s/n, Campus Universitário, 36570-900 Viçosa, MG, Brazil

[c]Leibniz Institute for Baltic Sea Research, Seestrasse 15, 18119, Rostock, Germany

Correspondence to: **Caik Oliveira de Miranda**
E-mail: caik.miranda@ufv.br

Author contributions

C. O. de Miranda – Conceptualization, Methodology, Formal analysis, Investigation, Writing (Original Draft, Review & Editing), Data Analysis, Visualization; C. E. G. R. Schaefer – Conceptualization, Supervision, Project Administration, Writing (Review & Editing); J. J. L. L. Souza – Conceptualization, Supervision, Writing (Review & Editing); L. M. Guimarães – Resources, Data Analysis; P. V. Sciamarella Maia – Resources, Data Analysis; J. A. Ivar do Sul – Conceptualization, Supervision, Writing (Review & Editing), Methodology.